Non-growing season methane emissions are a significant component of annual emissions across northern ecosystems

Claire C. Treat[1*], A. Anthony Bloom[2], Maija E. Marushchak[1]

[1] Department of Environmental and Biological Sciences, University of Eastern Finland, 70211 Kuopio, Finland

[2] Jet Propulsion Laboratory, California Institute of Technology, Pasadena, CA, USA

* Corresponding Author:
Claire C. Treat
Department of Environmental and Biological Sciences
University of Eastern Finland
70211 Kuopio
Finland
Tel: +358 469599744
Email: claire.treat@uef.fi

Article type: Primary research article

Running title: Annual and non-growing season CH_4 emissions

Index Terms and Key Words

Methane, wetlands, peatlands, tundra, boreal, non-growing season emissions, model-data comparison, synthesis

Abstract

Wetlands are the single largest natural source of atmospheric methane (CH_4), a greenhouse gas, and occur extensively in the northern hemisphere. Large discrepancies remain between "bottom-up" and "top-down" estimates of northern CH_4 emissions. To explore whether these discrepancies are due to poor representation of non-growing season CH_4 emissions, we synthesized non-growing season and annual CH_4 flux measurements from temperate, boreal, and tundra wetlands and uplands. Median non-growing season wetland emissions ranged from 0.9 g m^{-2} in bogs to 5.2 g m^{-2} in marshes and were dependent on moisture, vegetation, and permafrost. Annual wetland emissions ranged from 0.9 g m^{-2} y^{-1} in tundra bogs to 78 g m^{-2} y^{-1} in temperate marshes. Uplands varied from CH_4 sinks to CH_4 sources with a median annual flux of 0.0 ± 0.2 g m^{-2} y^{-1}. The measured fraction of annual CH_4 emissions during the non-growing season (observed: 13 to 47%) was significantly larger than was predicted by two process-based model ensembles, especially between 40-60º N (modeled: 4 to 17%). Constraining the model ensembles with the measured non-growing fraction increased total non-growing season and annual CH_4 emissions. Using this constraint, the modeled non-growing season wetland CH_4 flux from >40° north was 6.1 ± 1.5 Tg y^{-1}, three times greater than the non-growing season emissions of the unconstrained model ensemble. The annual wetland CH_4 flux was 37 ± 7 Tg y^{-1} from the data-constrained model ensemble, 25% larger than the unconstrained ensemble. Considering non-growing season processes is critical for accurately estimating CH_4 emissions from high latitude ecosystems, and necessary for constraining the role of wetland emissions in a warming climate.

Introduction

Methane (CH_4) is an important greenhouse gas with 33 times the radiative forcing of CO_2 (Myhre *et al.*, 2013). Wetlands are the largest natural source of methane, contributing an estimated 125 - 235 Tg CH_4 to the atmosphere annually (Saunois *et al.*, 2016). Model-based estimates of temperate, boreal, and tundra wetland CH_4 emissions at latitudes greater than 40º N amount to 16 – 36% of global wetland emissions (Melton *et al.*, 2013). However, large discrepancies remain between "bottom-up" emissions estimates using process-based or data-constrained models and "top-down" emissions estimates from atmospheric CH_4 measurement inversions (Kirschke *et al.*, 2013, Saunois *et al.*, 2016). Specifically, bottom-up wetland CH_4 emissions remain highly uncertain due to poorly constrained and highly divergent maps of wetland area, a high degree of uncertainty in CH_4 process parameterization, and lack of validation datasets (Melton *et al.*, 2013). Due to a relatively limited representation of wetland CH_4 emission process controls, bottom-up approaches to modeling CH_4 may be missing some important contributions of both non-growing season CH_4 flux (Xu *et al.*, 2016a, Zona *et al.*, 2016) and spatial variability in CH_4 emissions. Accounting for these factors may improve the agreement between top-down and bottom-up CH_4 emissions estimates (Kirschke *et al.*, 2013, Saunois *et al.*, 2016).

Recently, the importance of non-growing season CH_4 emissions to the annual budget was shown for several tundra sites, where non-growing season fluxes comprise ~50% of the annual emissions (Karion *et al.*, 2016, Mastepanov *et al.*, 2008, Zona *et al.*, 2016). However, the importance of non-growing season emissions over greater temporal and spatial scales is unclear. Continued measurements over several years at one tundra site showed that the high non-growing season CH_4 emissions measured in one year were anomalous and were not measured in any of the next four years (Mastepanov *et al.*, 2013, Pirk *et al.*, 2015). At a temperate wetland site, winter CH_4 measurements over multiple years showed that the non-growing season flux constituted a much smaller proportion (less than 10%) of the annual emissions (Melloh & Crill, 1996). These differing results could simply reflect spatial heterogeneities among sites, but also reflect a fundamental lack of understanding of what processes control non-growing season emissions (including in-situ CH_4 production, inhibition of CH_4 oxidation, release of CH_4 stored in peat, or some combination of the above) in both individual sites and across sites. Consequently, the role of non-growing season emissions in the annual wetland CH_4 budget remains highly uncertain.

Ecosystem CH_4 flux is the net result of CH_4 production in anaerobic soil minus CH_4 oxidation in aerobic soil (e.g. Blodau, 2002). Anaerobic CH_4 oxidation using alternative electron acceptors, such as sulfates, nitrates, iron, manganese, and humic substances, has been reported from freshwater systems (e.g., Segarra *et al.*, 2015), but its importance for CH_4 cycling is not yet understood. Rates of CH_4 production are dependent on temperature, pH, and the availability of substrate (e.g. Moore & Dalva, 1997, Treat *et al.*, 2015). However, CH_4 fluxes are highly unpredictable at daily time scales due to CH_4 oxidation and the variable time lag between CH_4 production and emission. Emissions can be closely coupled to CH_4 production due to efficient plant transport through aerenchymous tissue (King *et al.*, 1998), found in plants in the *Cyperacae* family, or decoupled due to slower diffusive transport and storage effects in anoxic soils (Blodau, 2002, Comas *et al.*, 2008, Pirk *et al.*, 2015). At the plot scale, CH_4 fluxes have been correlated with water table level, soil temperature, productivity, and vegetation composition (Bubier, 1995, Moore & Roulet, 1993, Whiting & Chanton, 1993). However, these relationships differ in strength depending on the time scales considered, with better correlations between environmental and plant controls on CH_4 at seasonal rather than at daily scales (Blodau, 2002, Treat *et al.*, 2007, Turetsky *et al.*, 2014). Furthermore, the spatial and temporal heterogeneity of CH_4 emissions can obscure broader trends among different wetland classes and biomes. Given a background of increasing CH_4 emissions from northern high latitudes (Nisbet *et al.*, 2014) and that wetlands are the largest natural source of methane (e.g. Saunois *et al.*, 2016), it is important to understand which types of wetlands and which regions (tundra, boreal, temperate) are potentially the largest contributors of CH_4 to the atmosphere as well as which have the greatest uncertainty. Taken together, an increasing number of CH_4 flux studies span a range of high-latitude ecosystems and provide a unique opportunity to advance current understanding of how net CH_4 emissions vary both spatially and temporally.

Here, we synthesize measurements of growing season, non-growing season, and annual CH_4 fluxes from temperate, boreal, and tundra wetland and upland ecosystems from 191 unique sites to determine the magnitude and controls of non-growing season CH_4 and annual emissions. Previous syntheses only explicitly considered CH_4 emissions during the growing season and generally only from wetlands (Bartlett & Harriss, 1993, Bridgham *et al.*, 2006, McGuire *et al.*, 2012, Olefeldt *et al.*, 2013, Turetsky *et al.*, 2014). We use our new synthesis dataset to: 1) identify trends in annual CH_4 emissions among tundra, boreal, and temperate wetlands and uplands; 2) identify the contributions of non-growing season flux to annual CH_4 emission; and 3) evaluate and constrain the seasonal timing and magnitude of CH_4 emissions for two process-based model ensembles [WETCHIMP (Melton *et al.*, 2013) and WetCHARTs (Bloom *et al.*, 2017)]. Together, the WetCHARTs and WETCHIMP model ensembles effectively provide a complimentary representation of uncertainty in global-scale model-based estimates of monthly wetland CH_4 emissions.

Materials and Methods

Data compilation

Annual, non-growing season, and growing season CH_4 flux measurements and ancillary data were synthesized from 174 published studies that made more than one measurement of CH_4 flux per month throughout the growing season (growing season) and more than two measurement during the non-growing season (non-growing season, annual). This resulted in 256 annual fluxes from 101 unique sites (including 48 unique sites with 131 explicitly differentiated non-growing season fluxes) and 853 growing season flux measurements from 191 unique sites (Fig. 1) made using static chambers, automated chambers, eddy covariance, and snowpack diffusion methods. Mean daily CH_4 flux, non-growing season and growing season CH_4 flux, and annual CH_4 flux were extracted from studies identified from Web of Science using the terms "methane" and "arctic" or "tundra" or "boreal" or "temperate", author knowledge, and from an existing synthesis dataset (McGuire *et al.*, 2012). For inclusion in the analysis of growing season and annual CH_4 fluxes, studies must have made more than one measurement of CH_4 flux per month throughout the growing season. For inclusion in the non-growing season CH_4 flux analysis, studies must have measured CH_4 flux more than twice during the non-growing season, defined as the period outside the photosynthetically active period. When this was not specifically defined within a study, the non-growing season included the period of mid-September through May at sites between 60º and 90º N, and November through March at sites between 40º N and 60º N.

For all studies, we included information on the site location (latitude, longitude), technique used (static/manual chamber, automated chamber, eddy-covariance), vegetation composition, and other descriptive variables. Where possible, we also extracted environmental variables including mean annual air temperature (n=540/853, 63%), mean annual precipitation (n=556/853, 65%), mean seasonal water table position (n= 621/853, 73%), where positive values indicate a flooded site, pH (n=338/853, 40%), and maximum active layer thickness (n=121/208 measurements in sites with permafrost, 58%). The descriptive categories included biome, wetland ecosystem classification, permafrost presence/absence, and categorical vegetation descriptions. Biome was extracted from Olson *et al.* (2001) using the site coordinates and included tundra, boreal/taiga, temperate, and other (montane grassland and shrubland, flooded grassland, subtropical). Landscape position information, hydrologic descriptions, soil type, and detailed vegetation descriptions were used to categorize the wetland ecosystem classes based on the Canadian Wetland

Classification system (Group, 1988). These categories included shallow water wetland (water depth < 2 m), marsh, swamp, fen, bog, and upland (including forest and grassland). The categorization of permafrost presence/absence was based on the presence or absence of permafrost in the measurement location or chamber as noted by the author and occurred in 52 sites representing 208 flux measurements. Categorical vegetation descriptions included classifying sites using the vegetation composition descriptions based on the dominance, presence (minor component), or absence of different categories of vascular vegetation: trees, shrubs, *Cyperacae* (including *Carex* spp. and *Eriophorum* spp.). The CH_4 flux synthesis data used in these analyses are archived and available for download from PANGAEA (https://doi.pangaea.de/10.1594/PANGAEA.886976).

Growing season and annual CH_4 emissions

If not given by the authors, we calculated cumulative CH_4 emissions for the growing season using several different approaches depending on the information included in the study, but generally from integrating the mean daily CH_4 flux over the entire growing season or summing the mean monthly CH_4 flux over the growing season. However, many sites did not include information on the length of the growing season. For these sites and unless otherwise stated by the authors, we assumed that the growing season spanned the full month of the beginning and end of the measurement period. Some authors modeled annual fluxes using empirical relationships; we used these for annual emissions when available (modeled fluxes, n= 47/853 measurements, Fig. 1). To calculate annual emissions from the cumulative growing season emissions when the authors did not measure or model the non-growing season flux (n= 551/853 measurements), the empirical relationship between cumulative growing season CH_4 flux and annual flux was used to estimate annual CH_4 flux (Table 1, Fig. S1). Estimated annual fluxes using cumulative growing season measurements ranged from

40% lower (fens) to 17% lower (uplands) to 11% lower (marshes) than measured annual fluxes on average, while this method resulted in substantially higher estimated annual fluxes than observed fluxes in bogs (400%) and shallow water wetlands (170%; Table S1). Some of this difference may be due to measurement bias in the annual measurements towards higher emitting sites and wetland classes (Table S3).

Comparison between modeled and measured growing season and annual CH_4 data

We use two recent wetland CH_4 emission model ensemble studies to evaluate model-based estimates of non-growing season and annual CH_4 emissions relative to measured values. The wetland CH_4 emission and uncertainty dataset for atmospheric chemistry and transport modelling (WetCHARTs) model ensemble approach (Bloom *et al.*, 2017) consists of 324 models with 0.5° spatial and monthly temporal resolution wetland CH_4 emission models, derived using a range of wetland extent maps, substrate availability models, mean global wetland CH_4 emissions factors, and temperature CH_4:C dependencies. The Wetland CH_4 Inter-comparison of Models Project (WETCHIMP) ensemble consists of six global-scale process-based models with monthly temporal and 0.5° - 3.6° spatial resolution with a range of prognostic and data-driven estimates of wetland extent and associated CH_4 emissions (Melton *et al.*, 2013). Together the WetCHARTs and WETCHIMP model ensembles represent a range of wetland CH_4 emission scenarios: the substantial range of modeled wetland CH_4 emission rates (which typically span more than one order of magnitude at sub-continental scales) are largely attributable to varying parameterizations of wetland extent and net CH_4 production processes across the WetCHARTs and WETCHIMP models. For the sake of brevity, we refer the reader to (Melton *et al.*, 2013) and Bloom *et al.* (2017) for additional details on the model structures. The two ensembles effectively provide a complimentary representation of uncertainty in global-scale model-based estimates of monthly wetland CH_4 emissions.

For the intercomparison of the timing of the CH_4 emissions between measured and modeled data, the growing season, non-growing season and annual wetland fluxes for all model ensemble members were summed within two latitudinal zones: 40° – 60° N and >60° N. For high latitudes (> 60° N), the growing season was defined as June through mid-September, while in lower latitudes (40° – 60° N), the growing season was defined as April – October. As the WetCHARTs model ensembles only represent wetland emissions and do not include CH_4 uptake or emission in upland soils, we included only measured non-growing season and annual CH_4 fluxes from wetland sites within our synthesis dataset in the model-data intercomparison. Evaluation of non-growing and annual CH_4 fluxes using zonal totals – instead of model gridcell evaluation – reduced biases introduced by the large number of grid cells with little or no wetland area and subsequently, negligible wetland CH_4 flux, as compared to the wetland subset of the synthesis dataset that exclusively contained CH_4 flux from wetland areas. We compared the synthesis and model datasets using the non-growing season fraction (non-growing season flux / annual flux).

Statistical Analysis

The non-growing season, growing season, and annual CH_4 flux data were not normally distributed, nor was the non-growing season fraction (non-growing season flux / annual flux). Here, we use the median and 95% confidence intervals around the median to describe the dataset. To calculate median and 95% confidence intervals for the measured and modeled flux data, we implemented bootstrap resampling in R (Team, 2008) using the “sample” command with replacement and determined the median for 10,000 simulations of resampled data. We used the maximum difference between median and interquartile range as the coefficient of variation when comparing variability among time scales and studies.

Linear mixed-effects modeling was used on the log-transformed measurement data to test for significant relationships between CH_4 fluxes and both categorical variables (biome, ecosystem class, dominant vegetation type, and presence/absence of permafrost) and continuous variables (growing season length, mean water table position, pH, soil temperature, mean annual temperature, and precipitation). Mixed-effects modeling was necessary because of the bias introduced from having multiple samples from the same site, resulting from measurements among distinct microtopographies and/or vegetation types, or measurements over several years (e.g. repeated measures, with sites). Thus, site was included as a random effect in the analyses. We implemented the mixed effects model using the lmer command from the lme4 package (Bates, 2010, Bates *et al.*, 2014, Bates *et al.*, 2015) for R statistical software (Team, 2008). The significance of the predictor variables were tested using a Chi^2 test against a null model using only site as a random variable (Bates *et al.*, 2015); both models were fit without reduced maximum likelihood. Interactions were tested for significance against additive models without interactions. We also used this approach to test the relationship between cumulative growing season and annual emissions for wetlands and uplands as separate categories (Table 1). Differences among categorical variables and regression parameters were determined from 95% confidence intervals of the model coefficients after re-fitting the model using the reduced maximum likelihood.

Results

Measured non-growing season CH_4 flux

We compared both the magnitudes of measured non-growing season CH_4 emissions and the fraction of annual emissions emitted during the non-growing season (non-growing season fraction = non-growing season emissions/annual emissions) for sites with year-round measurements (pink circles, Fig. 1). Non-growing season emissions ranged from -0.2 to 16.9 g CH_4 m^{-2} y^{-1} for wetland sites and -0.3 to 4.4 g CH_4 m^{-2} y^{-1} for upland sites. Non-growing season measurements were most common at bog and fen sites (n = 38 and 58, respectively), while less data were available from shallow aquatic ecosystems (n = 12), marshes (n = 19), swamps (n = 1), and upland sites (n = 8; Fig. 2c).

Non-growing season CH_4 emissions differed significantly among ecosystem classes ($Chi^2 = 46$, d.f. = 5, $P<0.0001$; Fig. 3a) but not among biomes ($Chi^2 = 0.9$, d.f. = 2, $P=0.63$; Fig. 3b). Median non-growing season CH_4 flux in fens and marshes was more than double the median emissions in bogs and uplands (Fig. 3a). The non-growing season fraction also varied significantly among ecosystem classes ($Chi^2=18.0$, d.f.=5, $P=0.003$; Fig. 3c). The median non-growing season fraction in upland sites was more than double the median non-growing season in fens and bogs and was smallest in marshes and shallow waters (Fig. 3c).

While the magnitude of non-growing season CH_4 emissions did not vary significantly across biomes (Fig. 3b), the non-growing season fraction did ($Chi^2 = 11$, d.f. = 2, $P=0.005$; Fig. 3d). The non-growing season fraction was largest in the tundra, averaging 42% (95% CI: 31- 48%) of annual emissions. In temperate sites, the non-growing season fraction was 20% (14 - 27%) of annual CH_4 emissions. In the boreal biome, the non-growing season fraction was significantly lower than the tundra and averaged 16% (12-17%) of annual emissions.

Environmental conditions had some effect on non-growing season emissions and the non-growing season fraction, especially the presence/absence of permafrost. Non-growing season CH_4 emissions from sites without permafrost were more than four times greater than from permafrost sites (2.7 ± 0.9 g CH_4 m^{-2} and 0.6 ± 0.4 g CH_4 m^{-2}, respectively; Fig. 4a). However, the non-growing season fraction in permafrost-free sites (17 ± 3%) was less than half than in permafrost sites (36 ± 16%; Fig. 4b). Water table position was positively correlated with the magnitude of non-growing season emissions, where drier sites had smaller non-growing season emissions than wetter sites (Fig. S2), but water table position was not a significant predictor of the non-growing season fraction (Chi^2 = 0.3, d.f. = 1, *P*=0.57). Mean annual temperature was a significant predictor of the non-growing season fraction, which was higher at colder sites (log(NGSF (%) + 1) = -0.054*MAAT + 2.925, Chi^2 = 6.7, d.f. = 1, *P*=0.01). While it is possible that the magnitude of non-growing season CH_4 emissions is related to the length of the non-growing season, this relationship was not statistically significant (Chi^2 = 1.1, d.f. = 1, *P*=0.30), nor was the relationship between the non-growing season fraction and the growing season length (Chi^2 = 0.3, d.f. = 1, *P*=0.56).

The cover of different vegetation types, when combined with permafrost, was a good predictor of non-growing season CH_4 fluxes. In permafrost-free sites, *Cyperacae*-dominated sites had larger non-growing season CH_4 emissions (5.2 ± 0.7 g CH_4 m^{-2}) than shrub-dominated sites (3.3 ± 0.9 g CH_4 m^{-2}) and tree-dominated sites (0.5 ± 0.7 g CH_4 m^{-2}); trends were similar in sites with permafrost but fluxes were 65-100% smaller (Fig. S3).In *Cyperacae*-dominated and tree-dominated sites, the non-growing season fraction did not differ between sites with and without permafrost (*Cyperacae*: 22% with vs 26%, without and with permafrost, respectively; Tree: 20% for both; Fig. S3) despite the strong overall trend of higher non-growing season fraction in permafrost sites.

Annual CH_4 fluxes

The dataset of annual CH_4 emissions included measured, modeled (by the original authors), and estimated (Table 1) annual emissions (Fig. 1). Annual CH_4 emissions generally followed a moisture, temperature, and nutrient gradient (Fig. 2b) and differed significantly among ecosystem types and biomes (Chi^2 = 107, d.f.=13, *P*<0.0001 for the interaction). Annual emissions ranged from -15 to 310 g CH_4 m^{-2} y^{-1} for wetland sites and -23 to 73 g CH_4 m^{-2} y^{-1}

for upland sites. CH_4 emissions from flooded and more nutrient rich sites, such as shallow waters, marshes, and fens, were greater or equal to emissions from bogs and upland sites (Fig. 2b). Among wetlands, temperate marshes were the largest CH_4 sources with a median flux of 78 (95% CI: 63-145) g CH_4 m^{-2} y^{-1} while tundra bogs were the smallest (0.9 g CH_4 m^{-2} y^{-1}; Table S1). Generally, median annual CH_4 fluxes from tundra wetlands were smaller (6.2 ± 1.7 g CH_4 m^{-2} y^{-1}) than boreal (7.2 ± 1.4 g CH_4 m^{-2} y^{-1}) or temperate (13.3 ± 5.4 g CH_4 m^{-2} y^{-1}) ecosystems (Fig. 2b, Table S1). However, upland CH_4 flux was similar across the biomes. Upland tundra sites were a very small net source of CH_4 annually, 0.04 g CH_4 m^{-2} y^{-1}, while upland temperate sites were a net sink of CH_4 (-0.4 g CH_4 m^{-2} y^{-1}, Table S1). The majority of measurements were made in the boreal region in nearly every ecosystem class (Fig. 2c).

Permafrost presence and dominant vegetation cover were also correlated with annual CH_4 emissions. Permafrost-free sites were larger CH_4 sources annually, emitting 2.5 times more CH_4 than sites with permafrost (6.9 vs. 2.7 g CH_4 m^{-2} y^{-1}; Fig. 4a). In permafrost sites, the relationship between active layer thickness and annual CH_4 flux was significant and positive (Fig. S4; $Chi^2 = 25$, d.f.=1, $P<0.0001$). In permafrost-free sites, *Cyperacae*-dominated sites had larger annual CH_4 emissions (23.7 ± 2.2 g CH_4 m^{-2} y^{-1}) than shrub-dominated sites (9.9 ± 1.1 g CH_4 m^{-2} y^{-1}) and tree-dominated sites (4.5 ± 2.1 g CH_4 m^{-2} y^{-1}); trends were similar in sites with permafrost but fluxes were 50-95% smaller (Fig. S3). The relationship between water table depth and annual CH_4 flux was positive and significant but explained little variance (Fig. S2).

Modeled and measured non-growing season fractions and flux magnitude

At mid-latitudes (40° to 60° N), the model ensemble means predicted a lower non-growing season CH_4 contribution to the annual emissions relative to the measured CH_4 fluxes. The median non-growing season fraction from the measured data between 40° - 60°N was 16.0%

(95% CI: 11.0 – 23.0%) of annual fluxes, substantially higher than the median from the combined model ensembles (Fig. 5a). For mid-latitudes in WetCHARTs, the modeled median non-growing season fraction was 4.7% (4.2-5.2%) and in WETCHIMP, it was 10.0% (6.2-17.0%) (Fig. 5a). The median total non-growing season emissions for the mid-latitude region between 40-60°N was 0.9 ± 0.2 Tg CH_4 y^{-1} in WetCHARTs and WETCHIMP combined (Fig. 6a; Table S2).

At northern latitudes (60° to 90° N), the two model ensembles performed better in representing the timing of the annual CH_4 emissions. The median non-growing season fraction in WetCHARTs was 15.8% (14.6-17.2%), while in WETCHIMP it was 22.9% (16.7 – 38.5%; Fig. 5b). The median non-growing season fraction from the measured data was intermediate: 17.0% (16.0-23.3%) of annual fluxes (Fig. 5b). The median total non-growing season emissions for the high-latitude region between 60-90° N was 1.0 ± 0.2 Tg CH_4 y^{-1} for WetCHARTs and WETCHIMP combined (Fig. 6b; Table S2).

Across both mid-latitudes (40° to 60° N) and northern latitudes (60° to 90° N), WetCHARTs and WETCHIMP model ensembles exhibited significant correlations between total non-growing season CH_4 fluxes and non-growing season fractions (r = 0.63 – 0.85, $P \leq 0.02$; Fig. 5a and 6b). We utilized the emergent relationship between modeled non-growing season fractions and fluxes to place a measurement-informed constraint on total CH_4 emissions from mid- and high-latitudes. For both spatial domains, we identified the model runs from the WetCHARTs and WETCHIMP model ensembles that fell within the 95% confidence intervals of the median measured non-growing season fraction (Fig. 6). Using this data-constraint, the resulting non-growing season flux from WETCHIMP and WetCHARTs was 4.5 ± 1.0 Tg CH_4 y^{-1} for wetlands in the region between 40 – 60° N, four times larger relative to the unconstrained emissions estimates (Fig. 6a; Table S2). For wetlands in the region between 60-90° N, the total data-constrained non-growing season emissions were 1.6

± 0.6 Tg CH_4 y^{-1}, 60% higher than the non-growing season emissions without the constraint. Based on the data-constrained model results, annual wetland emissions for 40-60º N amounted to 28.7 ± 4.7 Tg CH_4 y^{-1}, in contrast to 23.0 ± 2.0 Tg CH_4 y^{-1} in unconstrained model ensemble (Fig. S5a; Table S2). The annual wetland emission for >60º N amounted to 8.7 ± 2.8 Tg CH_4 y^{-1} in contrast to 6.8 ± 0.7 Tg CH_4 y^{-1} in the unconstrained model ensemble (Fig. S5b; Table S2). The observational constraint increased estimates of total annual wetland CH_4 emissions across all biomes > 40º N by 25%, from 29.8 ± 2.7 Tg CH_4 y^{-1} to 37.4 ± 7.2 Tg CH_4 y^{-1} (Table S2). This was due to higher estimated emissions during both the growing season (40% of increase) and non-growing season (60% of increase).

Discussion

The role of non-growing season emissions in annual CH_4 flux

This first attempt to synthesize the non-growing season emissions from pristine ecosystems of the northern hemisphere clearly shows that they are an important and non-zero component of annual emissions across all regions and ecosystem classifications (Fig. 3). Our results based on 131 measurements from 48 sites across the tundra, boreal, and temperate regions, generally agree with both of the conflicting observations that non-growing season emissions were and were not a large component of the annual budget (Alm *et al.*, 1999, Dise, 1992, Mastepanov *et al.*, 2008, Mastepanov *et al.*, 2013, Melloh & Crill, 1996, Zona *et al.*, 2016) by showing a substantial range in the non-growing season fraction among sites (Fig. 3c,d). The relative importance of the non-growing season emissions to annual budgets is largely driven by the magnitude of growing season emissions (Fig. S1), which vary more greatly in magnitude than non-growing season emissions (Fig. 3a,b, Table S3). Non-growing season emissions were generally larger from wet sites than dry sites, while the non-growing season fraction showed opposite trends (Fig. 3a,c). Nevertheless, non-growing season CH_4 fluxes were large enough that they cannot be discounted in measurements of annual emissions, especially in drier sites (Fig. 3).

On average, process-based models significantly underestimated the non-growing season fraction, especially in temperate and boreal regions (Fig. 5a). As a result, total non-growing season wetland emissions for 40-90º N from WETCHIMP and WetCHARTs were more than three times larger when the model results were constrained using the data (Fig. 6). The biased representation of non-growing season CH_4 emissions in process-based models and in atmospheric inversion frameworks can have a significant impact on continental-scale CH_4 budget estimates (Fig. 6; Thonat *et al.*, 2017, Xu *et al.*, 2016a) and lead to substantial biases in estimates of the role of wetland CH_4 carbon-climate feedbacks.

There is mounting evidence from atmospheric CH_4 concentration data of significant terrestrial emissions outside of the growing season (Karion *et al.*, 2016, Miller *et al.*, 2016, Sweeney *et al.*, 2016), but the magnitude of the flux is uncertain based on results from inversion and process-based models. Process-based models may curtail CH_4 production and emission too early relative to the time of soil freezing (Miller *et al.*, 2016), thus resulting in a seasonal emissions bias. Still, our unconstrained model estimates of non-growing season emissions from >60º N (1.0 Tg CH_4 y^{-1}) were significantly smaller than the 12 ± 5 Tg CH_4 y^{-1} recently estimated for arctic tundra wetlands and uplands (Zona *et al.*, 2016), and even with the data constraint, the non-growing season emissions from wetlands were only 1.6 ± 0.6 Tg CH_4 y^{-1} (Fig. 6b). Upland areas, not included to this model-data comparison, may or may not be an additional, significant CH_4 sources during the non-growing season (Lohila *et al.*, 2016, Zona *et al.*, 2016) since their fluxes were small but variable (0.0 ± 0.2 g CH_4 m^{-2}; Fig. 3a). Additionally, episodic CH_4 emissions, previously reported to occur, e.g., during soil freezing (Mastepanov *et al.*, 2008, Pirk *et al.*, 2015) as well as during the growing season, may have been missed in some studies due to low measurement frequency and are not well represented in process models. The differences between the models and the data (Figs. 5, 6) demonstrate the need to further investigate which process representations and parameterizations lead to modeled emission estimates that are in agreement with measured data.

Processes controlling non-growing season and annual emissions.

While the environmental and substrate controls favorable for high emissions during the growing season extend to the non-growing season, the processes responsible for non-growing season emissions seem to vary across the landscape. Non-growing season emissions in wetlands followed similar patterns to annual and growing season emissions and were related to moisture, temperature, and dominant vegetation (Fig. 2a,b, 3a,b, S2), as expected based on previous studies (Blodau, 2002, Bubier, 1995, Olefeldt *et al.*, 2013). The highest non-growing season and annual emissions were from wet sites rather than dry sites (Fig. 3a, S2), from *Cyperacae*-dominated sites without permafrost rather than sites with little vegetation, trees, and/or permafrost (Fig. S3a). Permafrost-free sites had 2.5 times larger CH_4 fluxes annually and four times larger fluxes during the non-growing season than their permafrost counterparts (Fig. 4a), a larger difference than previously observed in daily emissions during the growing season (Olefeldt *et al.*, 2013). This trend likely resulted from a tight coupling between soil temperatures and potential CH_4 production (Moore & Dalva, 1997, Treat *et al.*, 2015). . Furthermore, in sites with permafrost, annual fluxes were larger from sites with deeper active layers (Fig. S4) where warmer soils also result in a larger thawed soil volume, and with additional substrate available for decomposition (Levy *et al.*, 2012). These results suggest increased CH_4 emissions in future warmer climate from permafrost regions as soil temperatures warm and active layers deepen.

The relatively high non-growing season fraction in tundra as opposed to boreal and temperate ecosystems (e.g. Table 1, Fig. S1) may result from an interaction between soil temperature, vegetation, and substrate availability that potentially affect both rates of CH_4 production and oxidation. For example, several sub-arctic sites in discontinuous permafrost that were classified both as tundra (Stordalen, Seida) and boreal (Vaisjeäggi), had a relatively high non-growing season fraction (Bäckstrand *et al.*, 2010, Jackowicz-Korczyński *et al.*, 2010, Marushchak *et al.*, 2016, Nykänen *et al.*, 2003). These sites all have elevated permafrost bog surfaces, peat plateaus and palsas, where CH_4 emissions were very small (<0.1 g CH_4 m^{-2} y^{-1}), and adjacent low-lying, permafrost-free fens, which are hot spots of CH_4 emission in the heterogeneous landscape. Both the elevated peat plateaus and the low-lying fens had a high non-growing season fraction, ranging from 30% to 100% of annual emissions. However, the high non-growing season is likely the result of different processes in the drier and wetter sites. In the low-lying wetlands, snowpacks are often thicker than surrounding uplands and peat plateaus due to wind redistribution of snow to the low-lying areas where fens are found (Heikkinen *et al.*, 2002), resulting in warmer soil temperatures throughout the year to a greater depth in the soil, reflected in deeper active layers and/or the absence of permafrost (Blanc-Betes *et al.*, 2016). With persistent anaerobic conditions provided by ice cover near the surface, little variation in the water table during the winter, and temperatures often above 0º C, CH_4 production continues during the winter-time, albeit at slower rates (Juottonen *et al.*, 2008, Melloh & Crill, 1996, Treat *et al.*, 2015). Additionally, the low-lying fens are also often more productive (Bäckstrand *et al.*, 2010, Marushchak *et al.*, 2013), and may also receive substrate inputs (DOC) via lateral flow from elevated areas, potentially increasing substrate available for CH_4 production. This points to the importance of warmer temperatures deeper in the peat profile for non-growing season CH_4 production, which can be facilitated by factors such as thick snow-pack or sufficiently deep peat that result in warmer (thawed) peat at depth while surface peats may be colder or frozen, and may occur at a broader geographic range of sites.

The non-growing season fraction showed an opposite wetness trend than the flux magnitude: It was twice as large in dry upland soils as in wetlands (Fig. 3a,c). The high contribution of non-growing season emissions in uplands is in accordance with findings from several upland arctic tundra sites in Alaska (Zona *et al.*, 2016). In upland soils, wintertime methanogenesis may be promoted by low oxygen diffusion into the frozen soil resulting in anaerobic conditions and substrate enrichment of the liquid water phase in partly frozen soil (Teepe *et al.*, 2001). However, inhibition of CH_4 oxidation through oxygen limitation and colder surface soil temperatures could be an even more important reason for the high contribution of wintertime CH_4 emissions in upland soils, including mineral soils, peat plateaus, and permafrost bogs, that commonly show net uptake of atmospheric CH_4 during the growing season (Fig. 2b, 3c; Marushchak *et al.*, 2016, Nykänen *et al.*, 2003, Zona *et al.*, 2016). Importantly, the wintertime emissions can turn upland soils that are summertime CH_4 sinks to net CH_4 sources annually, which occurred in at least four sites in this study (Lohila *et al.*, 2016, Ullah & Moore, 2011). Detailed, process-level studies are needed to show the contribution of CH_4 production vs. oxidation to the seasonality of CH_4 dynamics in upland or dry soils.

Storage and subsequent release of CH_4 during the non-growing season, which can be seen as decoupling of CH_4 production and emission, is important in some permafrost tundra sites (FechnerLevy & Hemond, 1996, Pirk *et al.*, 2015). Our synthesis data implies that the storage and subsequent release of previously produced CH_4 during the non-growing season can be related to the presence of permafrost and differences in vegetation type (Comas *et al.*, 2008, Parsekian *et al.*, 2011). As a rule, the non-growing season fraction of CH_4 emissions was higher in permafrost sites than in sites without permafrost (Fig. 4b). The presence of permafrost likely limited the size of the soil gas reservoir and, as the volume of ice increased as the soil water froze, CH_4 was pushed out (Pirk *et al.*, 2015), leading to a higher fraction of non-growing season emissions in permafrost soils although the flux magnitude was still small (Fig. 4b). However, in *Cyperacae* dominated sites, permafrost had no effect on the non-growing season fraction (Fig. S3b). Efficient plant transport by *Cyperacae* reduces the lag time between CH_4 production and emission to the atmosphere, thus reducing the role of storage within the peat (King *et al.*, 1998, Parsekian *et al.*, 2011, Strom *et al.*, 2003).

Spatial and temporal variability in CH_4 emissions

As hypothesized, the predictability of CH_4 emissions improved with longer time-scales. Considering annual time scales instead of daily time scales reduced the variability of CH_4 fluxes within wetland classes from 57-290% (Olefeldt *et al.*, 2013) to 56 – 130% in this study. Furthermore, the variability in CH_4 flux was reduced at the annual time scale (median = 34%, range = 2 to 290%) compared with the cumulative growing season (median = 45%, range = 2 to 450%), indicating that storage and transport played a significant role in the decoupling of CH_4 production and emission across all sites. This significant decoupling has implications for both modeling and measurements. For modeling, using daily CH_4 flux measurements during the growing season to calibrate or validate process-based models may result in an underestimation of the net annual CH_4 flux due storage in the peat structure. Future measurements need to focus on processes, including CH_4 production, oxidation, and transport pathways throughout the year, rather than simply on measuring the net CH_4 flux at the peat surface.

In addition to the known temporal and spatial variability, measurement-associated errors and data gaps may also contribute to the variance in annual CH_4 emissions (e.g. Fig. 2a,b) and need to be considered when planning measurements outside of the non-growing season. Static chambers were most commonly used for measurements during both the growing season (734/853 measurements) and during the non-growing season (99/131 measurements). Static chambers have a number of drawbacks, including potentially overestimating annual fluxes when diurnal temperature variations are high (Friborg *et al.*, 1997, Yao *et al.*, 2009), which can be common during the shoulder seasons and in some continental and drier sites (Mikkelä *et al.*, 1995, Yao *et al.*, 2009). Static chambers also can miss ebullition fluxes. Additionally, the calculation of CH_4 fluxes based on a linear increase in concentration in chambers can underestimate the magnitude of CH_4 fluxes by ~30% (Pihlatie *et al.*, 2013). Automated chamber setups have higher temporal resolution, which improves both the flux response to temperature and can better capture ebullition fluxes (Goodrich *et al.*, 2011) but are more expensive to set up and maintain and can generally cover smaller spatial region than manual static chambers. Eddy covariance methods can be preferable for winter measurements due to the harsh winter conditions but frequently result in low coverage of data with acceptable quality despite high frequency measurements. Methodological advancements in eddy covariance, including developing methods for the continuous measurement of CH_4, are improving the reliability of measurements during the non-growing season (Goodrich *et al.*, 2016). Currently, there were too few measurements to assess whether there were systematic differences between measurement techniques during the non-growing season. While increasing precision in methane flux measurements helps to reduce uncertainty of northern wetland methane emissions, factors like uncertainty in wetland area may still hamper accurate flux estimates and must also be addressed (e.g. Bloom *et al.*, 2017, Melton *et al.*, 2013).

Upland sites present a particular challenge to measuring annual CH_4 flux. First, there are relatively few measurements of annual CH_4 flux in upland ecosystems (Fig. 2c), especially ones that explicitly differentiate the role of non-growing season emissions. Therefore, due to the low number of samples and high variability of emissions (Fig. 2a, b), magnitude of non-growing season fluxes should be treated with caution. Furthermore, many estimates in upland ecosystems (and some treed wetlands) are based only on measurements from the soil surface, rather than above the tree canopy, and thus may be missing CH_4 released through trees (Machacova *et al.*, 2016). Additionally, year-round measurements of CH_4 flux in uplands are not common (Fig. 2c) but wet periods in forests can result in net annual CH_4 emissions rather than uptake (Lohila *et al.*, 2016, Ullah & Moore, 2011).

Moving high latitude methane budgets forward

Nearly 25 years ago, Bartlett and Harriss (1993) used all available CH_4 flux data and wetland maps from Matthews and Fung (1987) to estimate that wetlands north of 45º emitted 34 Tg CH_4 y^{-1} with an additional 4 Tg CH_4 y^{-1} from upland tundra soils. Using data-constrained process-based models based on significantly more annual CH_4 flux measurements (Fig. 2c), we arrived at a similar answer (37 ± 7 Tg CH_4 y^{-1}) for wetland emissions north of 40º (Table S2), which is also in good agreement with inverse modeling estimates of wetland CH_4 flux of 39 Tg CH_4 y^{-1} from natural emissions sources north of 30° (Saunois *et al.*, 2016). In the 25 years since Bartlett and Harriss (1993), process-based studies have provided key insights into the role of environmental conditions (e.g. Blodau, 2002, and references therein, Olefeldt *et al.*, 2013), substrate (Hodgkins *et al.*, 2014, Strom *et al.*, 2003), microbes (McCalley *et al.*, 2014), transport pathways (Christensen *et al.*, 2003, FechnerLevy & Hemond, 1996, King *et al.*, 1998), and storage (Comas *et al.*, 2008, Parsekian *et al.*, 2011, Pirk *et al.*, 2015) in net ecosystem CH_4 flux, which are represented with varying degrees of success in process-based models (Xu *et al.*, 2016b). The relatively small number of model runs falling within the non-growing season fraction observational constraint (15-33%, Fig. 6, Table S2) indicate that there is still significant room for improvement in the representation of CH_4 flux in process-based models.

Although most models underestimate growing season emissions, further efforts are required to attribute the model mismatch to specific model parameterizations or process representations. The range of model mismatches is partially independent of model process complexity, since the WetCHARTs model structure is relatively simple (in contrast to the range of WetCHIMP models). Both WetCHARTs and WetCHIMP model ensembles have similar success in accurately replicating the non-growing season fraction observational constraint (Fig. 6, Table S3), suggesting parameter uncertainty alone is a prominent source of error. For example, many of the WetCHARTS models within the observational data-constraint (Fig. 6) exhibited a low anaerobic CH_4:CO_2 temperature sensitivity (Fig. S6), although other constraints on the WetCHARTs ensemble parameterizations did not exhibit any clear tendencies. Aside from these trends, we anticipate that accurate representation of non-growing season processes, such as "zero-curtain" period emissions (Miller *et al.*, 2016, Zona *et al.*, 2016) and ebullition processes (Mastepanov *et al.*, 2008, Pirk *et al.*, 2015) are likely to have a substantial impact on the timing of and magnitude of modeled CH_4 emissions at high latitudes, while uncertainties in the competing influences of winter-time temperature and wetland extent controls likely play a significant role on non-growing wetland CH_4 emissions at lower latitudes (Bloom *et al.*, 2017). Ultimately, further investigation on the mismatch between the spatial components of modeled and observed non-growing season CH_4 fluxes - particularly with respect to climate forcing and wetland type - are essential to reconcile observed and model representations of wetland CH_4 processes. However, simply improving the representation of CH_4 processes might not be sufficient to improve modeled CH_4 flux; substantial improvements to the representation of soil temperature may also be required due to the several-fold differences between permafrost- and permafrost-free wetlands that must be captured in order to accurately represent CH_4 flux (Fig. 4).

The lack of empirical understanding about the processes involved in non-growing season CH_4 flux directly hinders efforts to model non-growing season flux. In the future, detailed process studies should be conducted to gain not only a better understanding of the role of different mechanisms controlling the CH_4 emissions outside of the growing season, but also the quantitative representation of these processes. An increased use of laser instruments for year-round, high-frequency measurements should further clarify the role of episodic CH_4 emissions during freeze-up, winter thaw events (e.g. Mastepanov *et al.*, 2008), and the growing season, and should be combined with continuous measurements of peat temperatures throughout the profile as well as measurements of porewater CH_4 concentrations as an indicator of CH_4 production. These efforts should be coordinated between measurement and modeling approaches in order to improve the bottom-up estimates of CH_4 flux. Additionally, future CH_4 flux measurements should focus on understudied ecosystems, such as shallow water wetlands, marshes, and uplands, and measure regularly throughout the year. This is particularly important in order to detect changing magnitude and seasonality of CH_4 fluxes due to climate change against the background interannual variability in CH_4 flux (Miller *et al.*, 2016, Sweeney *et al.*, 2016), and important for understanding global emission trends of this important greenhouse gas.

Acknowledgements

We thank two anonymous reviewers for thorough and constructive comments on this manuscript. CT was supported by the Finnish Academy of Sciences CAPTURE Project and the National Science Foundation P2C2 Program (ARC-1304823). MEM was supported by COUP (Constraining Uncertainties in the Permafrost-Climate Feedback, EU JPI Project ID 70426, decision no. 291691). Part of this research was conducted at the Jet Propulsion

Laboratory, California Institute of Technology, under a contract with the National Aeronautics and Space Administration; funding for AAB was provided through a NASA Earth Sciences grant (#NNH14ZDA001N-CMS). We thank C. Voigt, J. Bubier, S. Juutinen, T. Larmola, and C. Biasi for helpful discussions.

References

Alm J, Saarnio S, Nykanen H, Silvola J, Martikainen PJ (1999) Winter CO2, CH4 and N2O fluxes on some natural and drained boreal peatlands. Biogeochemistry, **44**, 163-186.

Bartlett KB, Harriss RC (1993) Review and Assessment of Methane Emissions from Wetlands. Chemosphere, **26**, 261-320.

Bates D (2010) lme4: Mixed-effects modeling with R. pp Page, Madison, WI, Springer.

Bates D, Maechler M, Bolker B, Walker S (2014) lme4: Linear mixed-effects models using Eigen and S4. pp Page.

Bates D, Mächler M, Bolker B, Walker S (2015) Fitting Linear Mixed-Effects Models Using lme4. 2015, **67**, 48.

Blanc-Betes E, Welker JM, Sturchio NC, Chanton JP, Gonzalez-Meler MA (2016) Winter precipitation and snow accumulation drive the methane sink or source strength of Arctic tussock tundra. Global Change Biology, **22**, 2818-2833.

Blodau C (2002) Carbon cycling in peatlands- A review of processes and controls. Environmental Reviews, **10**, 111-134.

Bloom AA, Bowman KW, Lee M *et al.* (2017) A global wetland methane emissions and uncertainty dataset for atmospheric chemical transport models (WetCHARTs version 1.0). Geosci. Model Dev., **10**, 2141-2156.

Bridgham SD, Megonigal JP, Keller JK, Bliss NB, Trettin C (2006) The carbon balance of North American wetlands. Wetlands, **26**, 889-916.

Bubier JL (1995) The Relationship of Vegetation to Methane Emission and Hydrochemical Gradients in Northern Peatlands. Journal of Ecology, **83**, 403-420.

Bäckstrand K, Crill PM, Jackowicz-Korczyñski M, Mastepanov M, Christensen TR, Bastviken D (2010) Annual carbon gas budget for a subarctic peatland, Northern Sweden. Biogeosciences, **7**, 95-108.

Christensen TR, Panikov N, Mastepanov M *et al.* (2003) Biotic controls on CO2 and CH4 exchange in wetlands - a closed environment study. Biogeochemistry, **64**, 337-354.

Comas X, Slater L, Reeve A (2008) Seasonal geophysical monitoring of biogenic gases in a northern peatland: Implications for temporal and spatial variability in free phase gas production rates. Journal of Geophysical Research: Biogeosciences, **113**, n/a-n/a.

Dise NB (1992) Winter Fluxes of Methane from Minnesota Peatlands. Biogeochemistry, **17**, 71-83.

Fechnerlevy EJ, Hemond HF (1996) Trapped methane volume and potential effects on methane ebullition in a northern peatland. Limnology and Oceanography, **41**, 1375-1383.

Friborg T, Christensen TR, Sogaard H (1997) Rapid response of greenhouse gas emission to early spring thaw in a subarctic mire as shown by micrometeorological techniques. Geophysical Research Letters, **24**, 3061-3064.

Goodrich JP, Oechel WC, Gioli B, Moreaux V, Murphy PC, Burba G, Zona D (2016) Impact of different eddy covariance sensors, site set-up, and maintenance on the annual balance of CO2 and CH4 in the harsh Arctic environment. Agricultural and Forest Meteorology, **228–229**, 239-251.

Goodrich JP, Varner RK, Frolking S, Duncan BN, Crill PM (2011) High frequency measurements of methane ebullition over a growing season at a temperate peatland site. Geophys. Res. Lett.

Group NWW (1988) Wetlands of Canada. Ecological land classification series, no. 24. Sustainable Development Branch, Environment Canada, Ottawa, Ontario, and Polyscience Publications Inc., Montreal, Quebec, **452**.

Heikkinen JEP, Maljanen M, Aurela M, Hargreaves KJ, Martikainen PJ (2002) Carbon dioxide and methane dynamics in a sub-Arctic peatland in northern Finland. Polar Research, **21**, 49-62.

Hodgkins SB, Tfaily MM, Mccalley CK *et al.* (2014) Changes in peat chemistry associated with permafrost thaw increase greenhouse gas production. Proceedings of the National Academy of Sciences, **111**, 5819-5824.

Jackowicz-Korczyński M, Christensen TR, Bäckstrand K, Crill P, Friborg T, Mastepanov M, Ström L (2010) Annual cycle of methane emission from a subarctic peatland. Journal of Geophysical Research: Biogeosciences, **115**, n/a-n/a.

Juottonen H, Tuittila E-S, Juutinen S, Fritze H, Yrjälä K (2008) Seasonality of rDNA-and rRNA-derived archaeal communities and methanogenic potential in a boreal mire. The ISME journal, **2**, 1157-1168.

Karion A, Sweeney C, Miller JB *et al.* (2016) Investigating Alaskan methane and carbon dioxide fluxes using measurements from the CARVE tower. Atmospheric Chemistry and Physics, **16**, 5383-5398.

King JY, Reeburgh WS, Regli SK (1998) Methane emission and transport by arctic sedges in Alaska: Results of a vegetation removal experiment. Journal of Geophysical Research-Atmospheres, **103**, 29083-29092.

Kirschke S, Bousquet P, Ciais P *et al.* (2013) Three decades of global methane sources and sinks. Nature Geosci, **6**, 813-823.

Levy PE, Burden A, Cooper MDA *et al.* (2012) Methane emissions from soils: synthesis and analysis of a large UK data set. Global Change Biology, **18**, 1657-1669.

Lohila A, Aalto T, Aurela M *et al.* (2016) Large contribution of boreal upland forest soils to a catchment-scale CH4 balance in a wet year. Geophysical Research Letters, **43**, 2946-2953.

Machacova K, Bäck J, Vanhatalo A *et al.* (2016) Pinus sylvestris as a missing source of nitrous oxide and methane in boreal forest. Scientific Reports, **6**, 23410.

Marushchak ME, Friborg T, Biasi C *et al.* (2016) Methane dynamics in the subarctic tundra: combining stable isotope analyses, plot- and ecosystem-scale flux measurements. Biogeosciences, **13**, 597-608.

Marushchak ME, Kiepe I, Biasi C *et al.* (2013) Carbon dioxide balance of subarctic tundra from plot to regional scales. Biogeosciences, **10**, 437-452.

Mastepanov M, Sigsgaard C, Dlugokencky EJ, Houweling S, Strom L, Tamstorf MP, Christensen TR (2008) Large tundra methane burst during onset of freezing. Nature, **456**, 628-U658.

Mastepanov M, Sigsgaard C, Tagesson T, Ström L, Tamstorf MP, Lund M, Christensen TR (2013) Revisiting factors controlling methane emissions from high-Arctic tundra. Biogeosciences, **10**, 5139-5158.

Matthews E, Fung I (1987) Methane emission from natural wetlands: Global distribution, area, and environmental characteristics of sources. Global Biogeochemical Cycles, **1**, 61-86.

Mccalley CK, Woodcroft BJ, Hodgkins SB *et al.* (2014) Methane dynamics regulated by microbial community response to permafrost thaw. Nature, **514**, 478-481.

Mcguire AD, Christensen TR, Hayes D *et al.* (2012) An assessment of the carbon balance of Arctic tundra: comparisons among observations, process models, and atmospheric inversions. Biogeosciences, **9**, 3185-3204.

Melloh RA, Crill PM (1996) Winter methane dynamics in a temperate peatland. Global Biogeochemical Cycles, **10**, 247-254.

Melton JR, Wania R, Hodson EL *et al.* (2013) Present state of global wetland extent and wetland methane modelling: conclusions from a model inter-comparison project (WETCHIMP). Biogeosciences, **10**, 753-788.

Mikkelä C, Sundh I, Svensson BH, Nilsson M (1995) Diurnal variation in methane emission in relation to the water table, soil temperature, climate and vegetation cover in a Swedish acid mire. Biogeochemistry, **28**, 93-114.

Miller SM, Miller CE, Commane R *et al.* (2016) A multiyear estimate of methane fluxes in Alaska from CARVE atmospheric observations. Global Biogeochemical Cycles, **30**, 1441-1453.

Moore TR, Dalva M (1997) Methane and carbon dioxide exchange potentials of peat soils in aerobic and anaerobic laboratory incubations. Soil Biology & Biochemistry, **29**, 1157-1164.

Moore TR, Roulet NT (1993) Methane Flux - Water-Table Relations in Northern Wetlands. Geophysical Research Letters, **20**, 587-590.

Myhre G, Shindell D, Bréon F-M *et al.* (2013) Anthropogenic and Natural Radiative Forcing. In: *Climate Change 2013: The Physical Science Basis. Contributions of Working Group I to the Fifth Assessment Report of the Intergovernmental Panel on Climate Change. .* (eds Stocker TF, Qin D, Plattner G-K, Tignor M, Allen SK, Boschung J, Nauels A, Xia Y, Bex V, Midgley PM) pp Page. Cambridge, United Kingdom and New York, NY, USA, Cambridge University Press.

Nisbet EG, Dlugokencky EJ, Bousquet P (2014) Methane on the Rise—Again. Science, **343**, 493-495.

Nykänen H, Heikkinen JEP, Pirinen L, Tiilikainen K, Martikainen PJ (2003) Annual CO2 exchange and CH4 fluxes on a subarctic palsa mire during climatically different years. Global Biogeochemical Cycles, **17**, n/a-n/a.

Olefeldt D, Turetsky MR, Crill PM, Mcguire AD (2013) Environmental and physical controls on northern terrestrial methane emissions across permafrost zones. Global Change Biology, **19**, 589-603.

Olson DM, Dinerstein E, Wikramanayake ED *et al.* (2001) Terrestrial Ecoregions of the World: A New Map of Life on Earth: A new global map of terrestrial ecoregions provides an innovative tool for conserving biodiversity. Bioscience, **51**, 933-938.

Parsekian AD, Comas X, Slater L, Glaser PH (2011) Geophysical evidence for the lateral distribution of free phase gas at the peat basin scale in a large northern peatland. Journal of Geophysical Research: Biogeosciences, **116**, n/a-n/a.

Pihlatie MK, Christiansen JR, Aaltonen H *et al.* (2013) Comparison of static chambers to measure CH4 emissions from soils. Agricultural and Forest Meteorology, **171**, 124-136.

Pirk N, Santos T, Gustafson C *et al.* (2015) Methane emission bursts from permafrost environments during autumn freeze-in: New insights from ground-penetrating radar. Geophysical Research Letters, **42**, 6732-6738.

Saunois M, Bousquet P, Poulter B *et al.* (2016) The global methane budget 2000–2012. Earth Syst. Sci. Data, **8**, 697-751.

Segarra K, Schubotz F, Samarkin V, Yoshinaga M, Hinrichs K, Joye S (2015) High rates of anaerobic methane oxidation in freshwater wetlands reduce potential atmospheric methane emissions. Nature Communications, **6**, 7477.

Strom L, Ekberg A, Mastepanov M, Christensen TR (2003) The effect of vascular plants on carbon turnover and methane emissions from a tundra wetland. Global Change Biology, **9**, 1185-1192.

Sweeney C, Dlugokencky E, Miller CE *et al.* (2016) No significant increase in long-term CH4 emissions on North Slope of Alaska despite significant increase in air temperature. Geophysical Research Letters, **43**, 6604-6611.

Team RDC (2008) R: A language and environment for statistical computing. pp Page, Vienna, Austria, R Foundation for Statistical Computing.

Teepe R, Brumme R, Beese F (2001) Nitrous oxide emissions from soil during freezing and thawing periods. Soil Biology and Biochemistry, **33**, 1269-1275.

Thonat T, Saunois M, Bousquet P *et al.* (2017) Detectability of Arctic methane sources at six sites performing continuous atmospheric measurements. Atmos. Chem. Phys., **17**, 8371-8394.

Treat CC, Bubier JL, Varner RK, Crill PM (2007) Timescale dependence of environmental and plant-mediated controls on CH4 flux in a temperate fen. Journal of Geophysical Research-Biogeosciences, **112**, G01014.

Treat CC, Natali SM, Ernakovich J *et al.* (2015) A pan-Arctic synthesis of CH4 and CO2 production from anoxic soil incubations. Global Change Biology, **21**, 2787-2803.

Turetsky MR, Kotowska A, Bubier J *et al.* (2014) A synthesis of methane emissions from 71 northern, temperate, and subtropical wetlands. Global Change Biology, **20**, 2183-2197.

Ullah S, Moore TR (2011) Biogeochemical controls on methane, nitrous oxide, and carbon dioxide fluxes from deciduous forest soils in eastern Canada. Journal of Geophysical Research: Biogeosciences, **116**, n/a-n/a.

Whiting GJ, Chanton JP (1993) Primary Production Control of Methane Emission from Wetlands. Nature, **364**, 794-795.

Xu X, Riley WJ, Koven CD *et al.* (2016a) A multi-scale comparison of modeled and observed seasonal methane emissions in northern wetlands. Biogeosciences, **13**, 5043-5056.

Xu X, Yuan F, Hanson PJ *et al.* (2016b) Reviews and syntheses: Four decades of modeling methane cycling in terrestrial ecosystems. Biogeosciences, **13**, 3735-3755.

Yao Z, Zheng X, Xie B *et al.* (2009) Comparison of manual and automated chambers for field measurements of N2O, CH4, CO2 fluxes from cultivated land. Atmospheric Environment, **43**, 1888-1896.

Zona D, Gioli B, Commane R *et al.* (2016) Cold season emissions dominate the Arctic tundra methane budget. Proceedings of the National Academy of Sciences, **113**, 40-45.

Table 1. Relationship between cumulative growing season CH_4 flux (g CH_4 m^{-2}) and annual growing season flux (g CH_4 m^{-2}) from sites that were measured throughout the year using linear mixed effects modeling. The relationship differed significantly among biomes in wetlands and between sites with and without permafrost in uplands. Parentheses indicate standard error. Models were tested against a null model including additive effects of cumulative growing season and biome (wetlands) or permafrost presence/absence (uplands).

Class	**Slope**	**Intercept**	**n**
Wetlands			
Temperate	1.054 (± 0.018)	1.654 (± 0.775)	25
Boreal/Taiga	1.017 (± 0.028)	2.680 (± 0.468)	67
Tundra	1.486 (± 0.060)	0.178 (± 0.850)	25
	Chi^2=21.8, d.f.=4	*P*=0.0002	
Uplands			
No permafrost	0.816 ± 0.304	-0.346 ± 0.171	2
Permafrost	2.443 ± 0.431	-0.016 ± 0.036	6
	Chi^2=18.4, d.f.=2	*P*< 0.0001	

Fig. 1. Map of sites with annual CH_4 flux measurements (pink circles), sites with annual flux estimates based on the relationship of total growing season CH_4 flux and annual CH_4 flux (blue squares, Table 1), and sites where original authors modeled annual fluxes (green triangles). Borders of biomes/ecoregions used in the study are delineated (Olson *et al.*, 2001). Additional sites (n=18) are not shown due to missing coordinates.

Fig. 2. (a) Measured non-growing season CH_4 emissions, (b) measured, modeled and estimated annual CH_4 emissions, and (c) number of measurements among wetland categories and uplands for temperate, boreal/taiga, and tundra regions. Boxes represent 25th, 75th percentile of data, line represents median, whiskers denote 10th and 90th percentile of data. Note differing y-axis scales. Annual CH_4 fluxes include measured, modeled, and estimated fluxes (Methods, Table 1). (c) Total number of site x year measurements, including annual fluxes estimated from growing season measurements only (solid, n=853) plus sites measured during the non-growing season (shaded, n=131).

Fig. 3. The measured non-growing season CH_4 emissions (top) and non-growing season fraction of annual emissions among ecosystem classes and biomes. (a) Non-growing season CH_4 fluxes differed significantly among ecosystem classes (Chi^2=46, d.f.=5, P<0.0001); (b) Non-growing season CH_4 fluxes did not differ signficantly among biomes (Chi^2=0.9, d.f.=2, P=0.63); (c) non-growing season fraction differed significantly among ecosystem classes (Chi^2=18.0, d.f.=5, P=0.003), and (b) biomes (Chi^2 = 11, d.f. = 2, P=0.005). Letters indicate significant differences (α=0.05) among the groups.

Fig. 4. Differences between sites with and without permafrost in (a) measured growing season, estimated non-growing season (Chi^2=19, d.f. = 1, P<0.0001), and estimated annual CH_4 fluxes (Chi^2=34, d.f. = 1, P<0.0001); and (b) measured non-growing season fraction (Chi^2=13, d.f. = 1, P=0.0003).

Fig. 5. The cumulative distribution function of observations of the non-growing season fraction (non-growing season CH_4 flux/annual CH_4 flux, %) for wetlands in the regions of (a) 40 – 60° N and (b) 60 – 90° N. Points represent the cumulative data distribution of the non-growing season fraction for the model ensembles (WetCHART, WETCHIMP) and measured datasets (Wetland data, blue). Vertical lines and boxes represent the median and the 95% confidence intervals around the median for each dataset.

Fig. 6. The non-growing season fraction and the total non-growing season flux from the two model ensembles for (a) 40° - 60° N and (b) north of 60° N. The model ensembles are wetCHARTs (open circles; n=324) and wetCHIMP (orange diamonds; n=6). Each point represents wetland CH_4 emissions from a single process model. The gold point represents the unconstrained median among all models (Model est). The blue point represents the median of data-constrained model results (Data-const) after selecting the model results that fell within the 95% confidence intervals of the measured median non-growing season fraction (Fig. 5), indicated by the gray box. Upland tundra areas may constitute an additional source (Fig. 2a)(Zona *et al.*, 2016); this estimate is strictly from wetland areas (Methods).

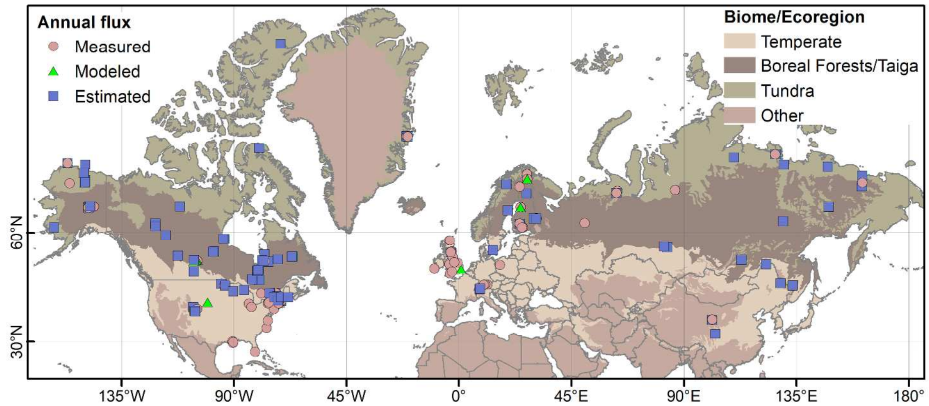

Figure 1. Map of sites with annual CH_4 flux measurements (pink circles), sites with annual flux estimates based on the relationship of total growing season CH_4 flux and annual CH_4 flux (blue squares, Table 1), and sites where original authors modeled annual fluxes (green triangles). Borders of biomes/ecoregions used in the study are delineated (Olson et al., 2001). Additional sites (n=18) are not shown due to missing coordinates.

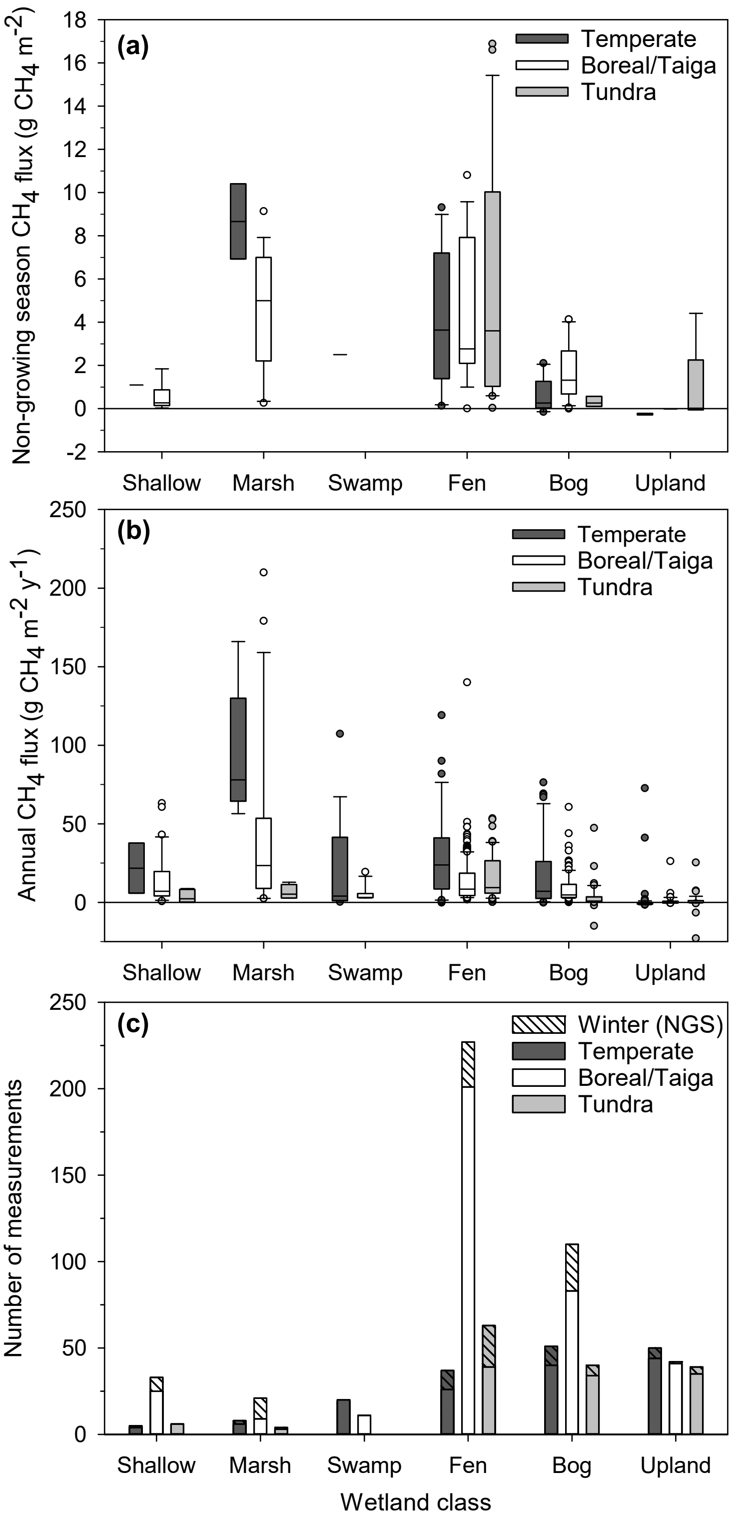
(a)
Temperate
Boreal/Taiga
Tundra
Non-growing season CH_4 flux (g CH_4 m^{-2})
Shallow
Marsh
Swamp
Fen
Bog
Upland
(b)
Temperate
Boreal/Taiga
Tundra
Annual CH_4 flux (g CH_4 m^{-2} y^{-1})
Shallow
Marsh
Swamp
Fen
Bog
Upland
(c)
Winter (NGS)
Temperate
Boreal/Taiga
Tundra
Number of measurements
Shallow
Marsh
Swamp
Fen
Bog
Upland
Wetland class

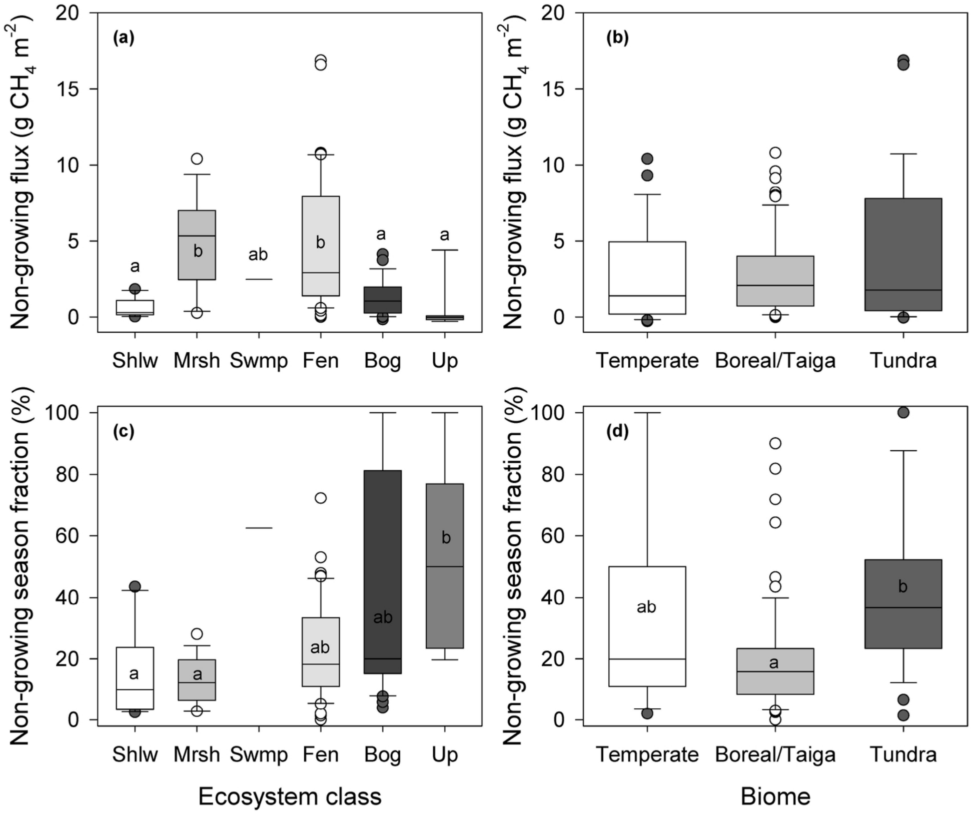

Figure 3. The measured non-growing season CH_4 emissions (top) and non-growing season fraction of annual emissions among ecosystem classes and biomes. (a) Non-growing season CH_4 fluxes differed significantly among ecosystem classes (Chi^2=46, d.f.=5, P<0.0001); (b) Non-growing season CH_4 fluxes did not differ significantly among biomes (Chi^2=0.9, d.f.=2, P=0.63); (c) non-growing season fraction differed significantly among ecosystem classes (Chi^2=18.0, d.f.=5, P=0.003), and (d) biomes (Chi^2 = 11, d.f. = 2, P=0.005). Letters indicate significant differences (α=0.05) among the groups.

165x138mm (300 x 300 DPI)

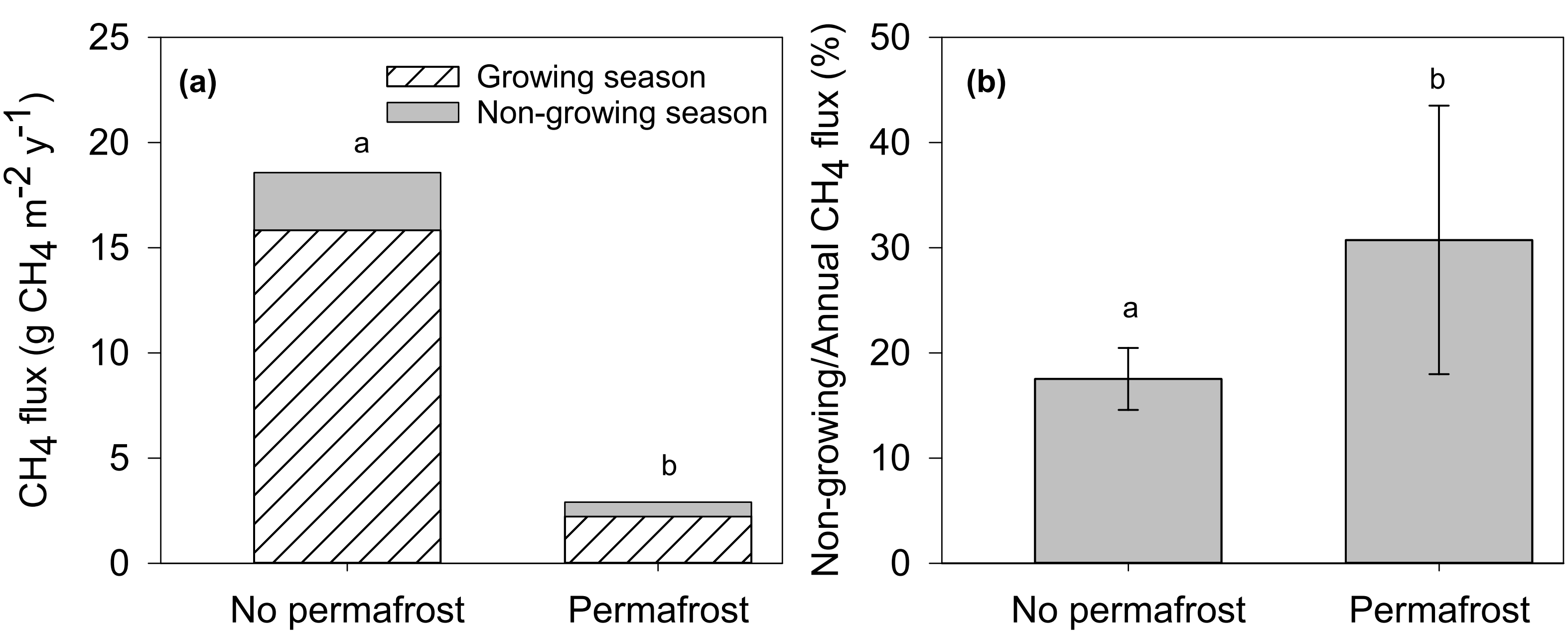

(a)
Growing season
Non-growing season
a
b
25
20
15
10
5
0
CH_4 flux (g CH_4 m^{-2} y^{-1})
No permafrost
Permafrost
(b)
a
b
50
40
30
20
10
0
Non-growing/Annual CH_4 flux (%)
No permafrost
Permafrost

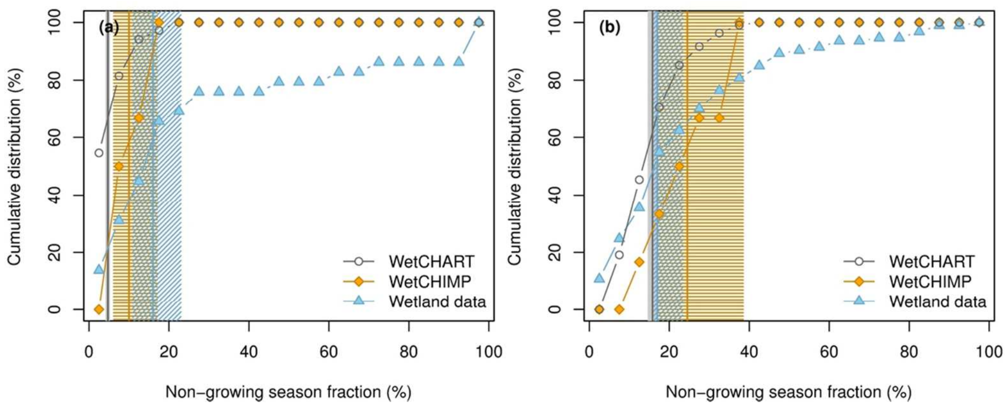

Fig. 5. The cumulative distribution function of observations of the non-growing season fraction (non-growing season CH4 flux/annual CH4 flux, %) for wetlands in the regions of (a) 40 – 60° N and (b) 60 – 90° N. Points represent the cumulative data distribution of the non-growing season fraction for the model ensembles (WetCHART, WETCHIMP) and measured datasets (Wetland data, blue). Vertical lines and boxes represent the median and the 95% confidence intervals around the median for each dataset.

101x40mm (300 x 300 DPI)

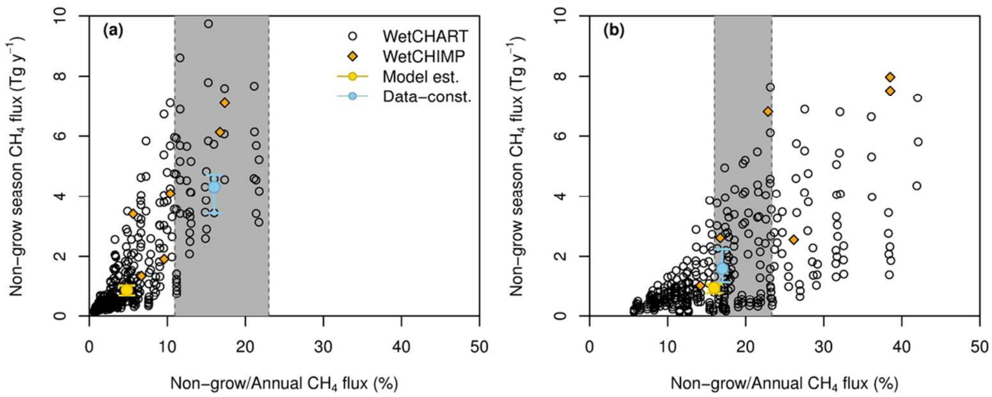

Figure 6. The non-growing season fraction and the total non-growing season flux from the two model ensembles for (a) 40° - 60° N and (b) north of 60° N. The model ensembles are wetCHARTs (open circles; n=324) and wetCHIMP (orange diamonds; n=6). Each point represents wetland CH_4 emissions from a single process model. The gold point represents the unconstrained median among all models (Model est). The blue point represents the median of data-constrained model results (Data-const) after selecting the model results that fell within the 95% confidence intervals of the measured median non-growing season fraction (Fig. 5), indicated by the gray box. Upland tundra areas may constitute an additional source (Fig. 2a)(Zona et al., 2016); this estimate is strictly from wetland areas (Methods).

101x40mm (300 x 300 DPI)